PHYSICAL REVIEW B VOLUME 22, NUMBER 2 15 JULY 1980

Configurational switching and charge transfer for optically excited rare-gas adsorbates on simple-metal surfaces

J. A. Cunningham, D. K. Greenlaw, and C. P. Flynn
Physics Department and Materials Research Laboratory, University of Illinois at Urbana-Champaign, Urbana, Illinois 61801

(Received 26 December 1979)

Optical spectra in the range 5–17 eV for rare-gas atoms adsorbed on simple-metal surfaces are reported. Various features in the spectra are coverage dependent presumably owing to interactions among adsorbates. The results reveal an important new process of charge transfer induced by the optical excitation. The observed spectra fall into one of two clearly distinct categories. In one of these the rare-gas spectrum at low coverage persists in a form resembling that of the rare-gas solid, but with a noticeable broadening and shifting of prominent features. In the other, the threshold is blue shifted by several eV into a shoulder lacking analogs of the exciton lines. The demarcation between these forms occurs close to the condition $I^* = \phi$ at which the excited-state ionization energy I^* equals the substrate work function ϕ. Near this point the excited rare gas becomes unstable against charge transfer to the surface. Results are interpreted as indicating charge transfer induced by the optical process. The mechanism switching the system between configurations appears sharp to ~ 0.1 eV in I^* or ϕ. Evidently the hopping matrix element connecting an excited electron on the rare gas to the bulk must be large (several eV). The observed line shapes for the cases of persistent spectra are difficult to understand in detail.

I. INTRODUCTION

Rare-gas atoms adsorb on metal surfaces to form surface complexes having unusually simple structures. This is the case for both the ground state and the lower-lying electronically excited configurations of the complex. In its ground state, a rare-gas atom has an inert (np^6) outer shell which interacts with the metal mainly through polarization mechanisms. Typical binding energies are $\lesssim 0.3$ eV. The lowest excited states of rare-gas atoms are not strongly mixed with the ground state by the surface perturbation. They are derived from $np^5(n+1)s$ structures. These excited configurations also behave in a chemically simple way on metal surfaces. Their chemical properties resemble those of their $np^6(n+1)s$ alkali neighbors in the Periodic Table to a remarkable degree, mainly because the nodal structures and binding energies of the s valence orbitals are almost identical in the two cases. It is this fortunate combination of simple ground- and excited-state properties that makes the rare gases particularly well suited to a fundamental investigation of electronically excited adsorbate-metal complexes.

Ehrlich and Hudda[1] and Gomer[2] confirmed Mignolet's[3] discovery that adsorbed rare-gas monolayers can cause significant decreases (~1 eV) in metal work functions. These results have been confirmed by a body of later work.[4] Related to the surface dipole effect is a binding enthalpy that increases, like the work function change, with rare-gas polarizability.[5] The division of this energy between correlation[6] (dispersion) and static (surface field) polarization[1,2] has been the center of much debate, as yet lacking unambiguous resolution.

By comparison to the excitation energies ~10 eV, and the shifts ~1–4 eV of interest here, these rare-gas couplings to the surface in the ground configuration are of minor significance. The important processes concern an instability of the *excited* configuration. This instability causes energy splittings an order of magnitude larger than the ground configuration bonding energy.[7]

The present work was undertaken as part of an ongoing exploration of the excitation characteristics of adsorbates coupled to metal surfaces. Prototype systems like the rare gases on simple metals have a particular value for an initial investigation of this type because the identity and character of the ground and final states are often easily established. A semiquantitative analysis may then suffice to identify new processes unambiguously. This is particularly important when quantitatively reliable theories are not yet available. Recent photoemission studies by Horn *et al.*,[9] for example, identify Xe excitations on Pd and probe the surface dispersion relation for the Xe adsorbate $5p$ band in monolayer films. These and earlier authors assume without further comment that photoemission leaves an adsorbed rare-gas atom ionized. In what follows we show that this assumption, while correct for particular cases, is not always valid.[7]

In the present work, the rare gases adsorbed on simple metals are employed to examine a specific charge-transfer process that takes place in certain cases between the adsorbate and substrate during an optical excitation. Rather similar processes have recently been reported by Avci and Flynn[8] for halogens dissolved in alkali metal hosts. A clear physical insight into the origin of the charge transfer in the case of present interest can be gained from the analogy mentioned above between alkali atoms and excited rare-gas atoms, together with Langmuir's classic discovery[10] that alkali atoms adsorb as positive ions on certain substrates. Taken together, these suggest that rare gas adsorbates take *neutral* alkali-like excited configurations in some instances, whereas *ionized* excited rare-gas configurations are expected in others. The spectral instability on which the present research is focused arises directly from the existence of these alternative excited configurations.

It has not yet proved possible to calculate most surface or adsorbate properties in an accurate way. Some basic features of simple-metal surfaces have been established by the density functional method augmented by pseudopotential theory[11] to the extent that reasonable work functions and surface energies are predicted.[12] Efforts have been made to apply similar methods to the adsorbate-surface complex.[13] More complicated metallic and compound surfaces (e.g., the transition metals) may better be dealt with directly by unrestricted Hartree-Fock methods,[14] which are also more aptly suited to adsorbate calculations.[15]

A general and more phenomenological approach will suffice for the present purposes. We shall need only the fact that electrons are bound into a metal by the work function ϕ and into an atom by an appropriate ionization potential I. Under conditions of relatively weak surface-to-atom coupling it may be anticipated that these descriptions of the separate parts maintain a substantial degree of validity in the composite coupled system. For example, a simple expectation[9] is that the surface complex finds its lowest energy with the atom ionized if $I < \phi$. This perception must be modified by the inclusion of the difference between the interaction energies in the two configurations in order to be accurate when the atom is close to the surface.

Within this approach we recognize that the same types of energy balance also occur in the excited configuration. This is the case whenever the excited configuration persists for a lifetime that is long compared with the plasmon period of the metal substrate[16] ($\sim 10^{-16}$ sec), which holds true almost invariably. The point is that excited configurations which satisfy the lifetime criterion must be self-consistent, with all electric fields appropriately screened in the metal. For this reason it is not, in general, possible for all types of excited atoms in contact with any particular metal to exist as ions. Criteria connected with local energy levels in the atom and metal, and with the electron-transfer rate between the two, determine which excited configuration occurs in practice. For example, it is not possible to excite an Na atom on the surface of an Na crystal into a self-consistent ionized configuration because the band electrons can simply flow to neutralize the ion. It is equally impossible for an excited rare-gas atom in an alkali-like configuration to be ionized on an alkali metal surface. On W, however, excited Xe (i.e., Xe*) must behave very much like Cs. It therefore exists in the Xe* $(5p^5)^+$ self-consistent configuration. This example is evidently consistent with the ionic structures assumed in the photoemission work,[9] whereas the case of an alkali metal surface mentioned above is not. A variety of metal-surface–rare-gas adsorbate complexes of both the ionic and the neutral type are examined in the present experimental investigations.

Surface reflectance spectroscopy (SRS) was chosen as the appropriate experimental technique for this work. The required range of photon energy and flux made the use of a synchrotron radiation source mandatory. From earlier experience[17] in the energy range $4 \lesssim \hbar\omega \lesssim 12$ eV it appeared certain that a spectroscopic sensitivity for adsorbate excitations comparable with that obtained in photoemission experiments could be achieved provided that a sufficiently stable two-beam method, compatible with ultrahigh vacuum requirements, could be developed for use with radiation in the range $4 \lesssim \hbar\omega \lesssim 25$ eV. In the absence of transparent media for use above 12 eV, beam splitting and coding must obviously be carried out by reflection. Furthermore, to avoid the need to prepare free-standing thin samples, it was necessary to employ a reflection spectroscopy. Details of the surface reflectance equipment developed, with an apparent stability ~1 in 10^5 for this purpose, are presented in Sec. II of this paper.

Surface reflectance spectra of submonolayer coverages cannot, at present, be interpreted unambiguously in terms of complex polarizabilities assigned to the adsorbed atoms. In the first place the surface layer of the *perfect* crystal undoubtedly has different optical properties from the bulk, and therefore makes a characteristic contribution to the reflectivity. Even in the absence of absorption, an adsorbate must shadow this surface layer and therefore partially mask its contribution to the reflectivity. Again, the adsorbate interacts with the surface layer to modify these properties in different ways for the ground and excited configurations. These properties of the substrate therefore also enter into the observed reflection (or transmission) spectra.

A classical theory of reflectivity changes induced by thin overlayers has been given by McIntyre and Aspnes[18] (MA). Experience with this theory has convinced us that, while valid and useful for thick (bulk) films, the theory has only a semiquantitative significance for monolayer films and is in fact, nonphysical for submonolayer coverages. These conclusions are generally consistent with those of other workers.[19] The main problem is that the classical treatment models even dilute submonolayer coverages as uniform slabs with thickness d and dielectric constant $\hat{\epsilon}$ ($\hat{\epsilon} = \epsilon_1 + i\epsilon_2$). For $d \to 0$ and s-polarized light the perturbation introduced by the surface layer does enter the final expression[18] for the reflectivity as $(\epsilon_2 - 1)d$, i.e., in proportion to the total added optical susceptibility. This appears appropriate for the simplest models in which the added layer has no effect on the properties of the underlying substrate. Even this requirement does not seem to be satisfied for p-polarized light.[18] Feibelman[20] has pointed out, in addition, that the extended interface region of real metals influences the boundary conditions in a significant way. The case of s-polarized light therefore seems considerably simpler than the p-polarized case, which is used in much of the present work for reasons of sensitivity. Some illustrative examples showing the use of the MA approach in this energy range are given in the Appendix.

In Sec. II, details of the equipment, its operation, and the experimental procedures are provided. The results obtained for rare gases adsorbed on metals are presented in Sec. III and interpreted in Sec. IV.

II. APPARATUS

A. Basic design

One of the principal constraints on the present work was the need to prepare accurately determined surface coverages of rare-gas adsorbates on simple metal substrates held in ultrahigh vacuum. It was desirable to maintain the substrate near liquid-He temperatures, both in order to obtain a unit sticking probability for precise doping and to eliminate all subsequent thermal desorption and surface diffusion. The necessary complication of cryogenic parts enclosing the substrate region, together with the desire to use ultraclean simple-metal surfaces, such as Al, Mg, and the alkali metals, then led to a choice of polycrystalline substrates evaporated *in situ* rather than single-crystal surfaces. The price paid for this choice is considerable: The surface geometry is complicated and poorly characterized. The degree to which this complication modifies the spectra of surface atoms is also not known. It appears quite possible that the energy balances examined in this work are insensitive to detailed surface geometry for simple metals. Nevertheless, further work employing single crystals will clearly be needed in order to determine the influence of surface geometry.

The basic experiment was a comparison of light reflected from a clean surface with that reflected from an identical surface supporting a carefully determined adsorbate coverage. In practice, a single freshly evaporated surface was used. Two optical beams were reflected from separate areas of this substrate. After an initial scan to determine imbalances between the two channels, one area—the sample area—was doped with adsorbates from a molecular beam while the other—the reference area—was left clean. A second scan was then made to determine the change in reflectance introduced by the adsorbates. An important part of this system is the beam splitting chopper that splits light from the monochromator into two stable beams. This chopper is described in Sec. IIB below. The vacuum chamber and cryohead are discussed in Sec. IIC and the optical system and the sample preparation procedures in Secs. IID and IIE, respectively. Some results that demonstrate the sensitivity of the equipment are presented in Sec. IIF.

B. Chopper

Four mirrors of gold-plated glass were employed to switch a light beam emerging from one of the Stoughton Seya-Namioka monochromators alternately between the sample area and the reference area of the substrate. Two mirrors were beveled and joined to form a 30° knife edge as shown in Fig. 1. Two additional mirrors were held at fixed spacings from the first pair. Light from the monochromator was focused at the knife edge. It is clear that the light is switched from one optical path to a second, parallel path as the assembly moves in such a way that the knife edge passes laterally through the focus. Approximately 30% of the incident light was transmitted by the two s-polarized reflections from the Au surfaces.

A number of different mountings for the basic

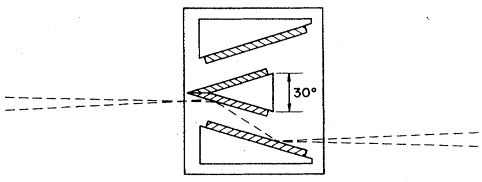

FIG. 1. Details of the chopper with the incident photon beam switched to an appropriate channel.

chopper might possibly be chosen. In the present work the mirror assembly was mounted on a self-oscillating stainless steel cantilever with $Q \sim 100$, electromagnetically driven by means of solenoids external to the vacuum bell jar. These coupled to Ni slugs on the chopper. A bounceless switch made and broke a circuit as the oscillator passed through zero displacement in the two alternative directions, and the current, when amplified, sustained the self-oscillations. Capacitative coupling between the vibrating mechanical oscillator and a nearby fixed pickup plate frequency modulated a tuned circuit. This modulation was used to amplitude-stabilize the chopper by feedback to the current amplifier driving the coils.

C. Vacuum chamber and cryohead

Conventional ultrahigh-vacuum techniques were used in this work to maintain the samples contamination-free. The bell jar was constructed in the MRL machine shop from 316 stainless steel. Copper gaskets were used throughout. The system was evacuated using ion pumps, turbomolecular and sorption pumps. After bakeout the pressure fell to 1×10^{-10} torr in the main bell jar. Much smaller pressures must exist inside the He temperature cryobaffles; no sample contamination could be detected over the course of many hours when the shutters were closed.

In the sample chamber layout, shown in Fig. 2(a), light from the chopper entered the cryohead through slots in the two Cu radiation shields and was reflected from the substrate in either s or p polarization, as chosen by a rotation of the sample assembly. After reflection, the light passed out of the cryohead through other slots to fall on viewports internally coated with sodium salicylate phosphor. The resulting luminescence was detected by a photomultiplier. The bell jar was also fitted with evaporation sources, with which fresh metal films could be prepared, and an appropriate baffled molecular beam source to deposit gas on the sample area. Equipment to monitor the metal and gas fluxes was also located in the bell jar.

Substrates on which samples could be prepared were held on a Cu block attached by Cu braid to the inner of two Cu radiation shields mounted on the Helitran cryptip [see Fig. 2(b)]. The substrate itself was made from sapphire brazed to Nb sheet. In this way the sample could be maintained at liquid-He temperatures. The block was mounted on an axle having positive stops at two orientations corresponding, respectively, to s and p reflections at 52° angles of incidence. In addition to the slots required for the transmission of the light beam, the two radiation shields were fitted with larger ports, having cold shutters which were actuated externally, through which the molecular beams passed during sample preparation. The shutters were invariably closed after sample preparation in order to screen the surfaces under examination from the ambient vacuum of the bell jar.

D. Signal detection and processing

A photomultiplier tube outside the bell jar was used to detect light from a phosphor coating on the inside of a window. In general, it proved necessary to rotate the tube until it exhibited equal sensitivities to the signal and reference beam channels. This was effected prior to a background scan which measured any residual asymmetries between the two channels (typically ~1% in operation) as a function of incident photon energy. The ratio (S/R) of light intensities in the signal and reference channels was stored. Without modification of the optical system, an adsorbed layer was

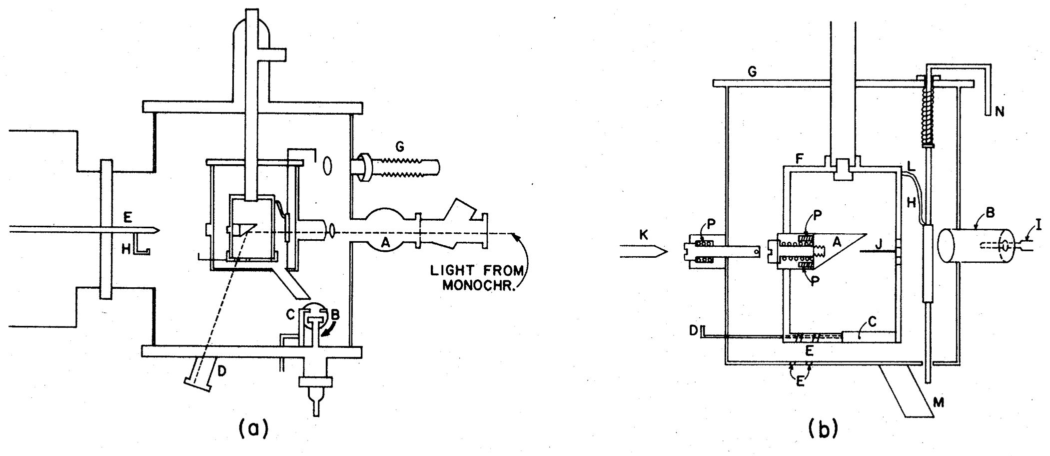

FIG. 2. (a) Assembly view of apparatus. Notice optical path for s-polarized reflection from sample. (b) Details of cryogenic system. The sample is located in the s-polarized configuration.

then prepared on the substrate and and new ratio $(S/R)'$ of channel intensities determined as a function of photon energy. The fractional change in reflectivity caused by adsorbates is

$$\frac{\delta S}{S} = \left(\frac{S}{R}\right)'\left(\frac{R}{S}\right) - 1 .$$

We note that both source and detector drifts are eliminated from the measured result by this method.

In practice, the *difference* of signals between the two channels was determined by phase-sensitive detection of the ac component of the photomultiplier output. This was divided by the mean signal to obtain the fractional difference using the ratiometric mode of a digital multimeter. The BCD output of this instrument was fed directly to a TI 960 computer. The computer stored and manipulated the data, and output the data to a chart recorder. It also controlled data acquisition and the monochromator advance.

E. Sample preparation

Samples were prepared only after the vacuum chamber had been baked, and runs were initiated immediately after sample preparation in order to avoid needless contamination. Previously outgassed boats pressed from tungsten, stainless steel, tantalum or niobium sheet, as appropriate, were used for metal evaporation. Quartz crystals held at low temperature were used to monitor the flux during evaporation. These readings were calibrated in auxiliary experiments by direct comparison with crystals held on the substrate itself.

Molecular beams of gases were directed to the sample by copper tubes leading from a capillary nozzle fed by clean gas at a predetermined pressure.[21] Prior measurements were made to determine the flux reaching the substrate in terms of the gas pressure across the nozzle. The gas and metal entered by separate ports, each equipped with a cold shutter which remained closed other than during sample preparation.

F. Optical Sensitivity

Figures 3(a) and 3(b) show the surface sensitivity that can be achieved by the present methods using light from the Tantalus I storage ring. In Fig. 3(a), the fractional reflectively change caused by

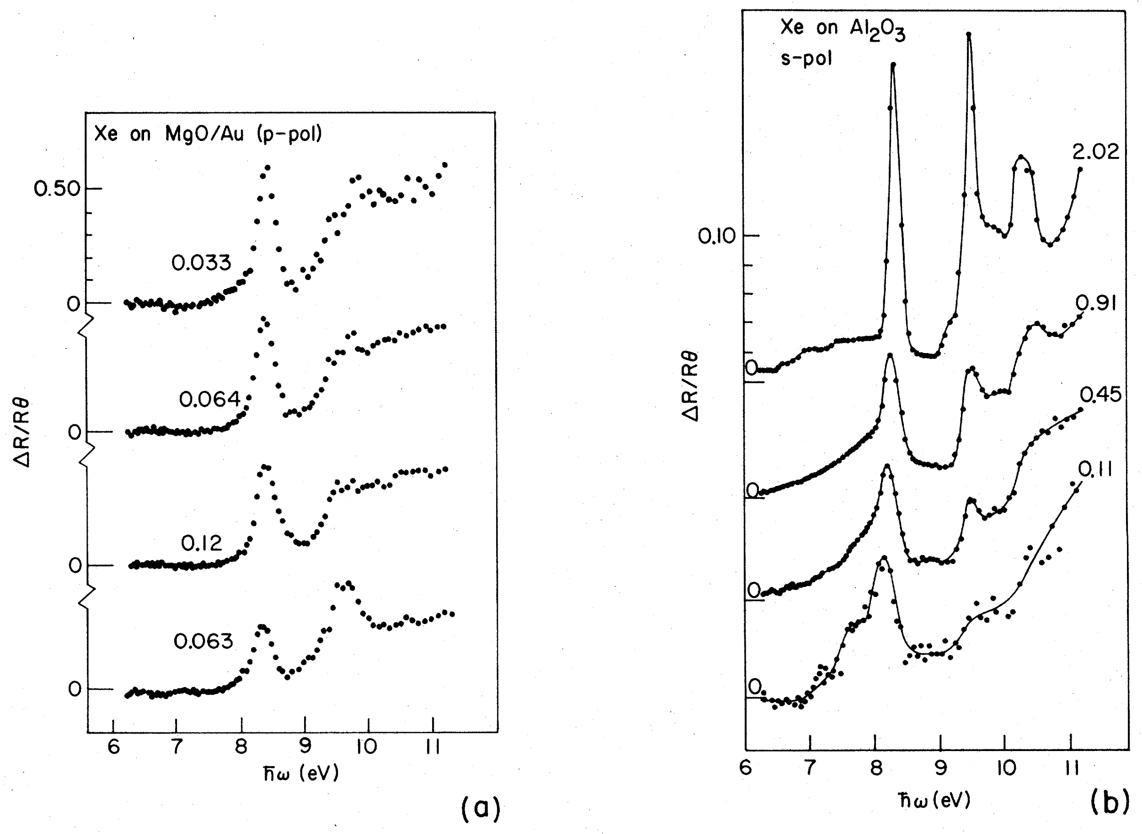

FIG. 3. (a) *p*-polarized reflectivity spectra (normalized to unit coverage) for Xe adsorbed on a substrate of MgO supported by gold. The bottom curve is for a 130-Å thick MgO layer, while the upper three were obtained for a 220-Å thick film. (b) *s*-polarized reflectivity changes for Xe adsorbed on Al_2O_3.

various coverages of Xe on MgO with p-polarized light is shown as a function of photon energy. Fig. 3(b) gives analogous results for Xe in Al_2O_3 with s-polarized light. In both cases, the sample was prepared by direct oxidation of evaporated metal in the bell jar. Since the surface structure is uncertain, the results are of value principally as illustrations of the available sensitivity. The sensitivity of the reflection signal to substrate properties also is displayed in Fig. 3(a) by the different Xe signals observed with MgO films, 130 and 220 Å thick.

Figure 3(a) demonstrates that ~0.03 monolayer of Xe on MgO can be observed at a signal-to-noise ratio of ~40 : 1 at the first exciton line near 8 eV. A somewhat smaller sensitivity is observed for Xe on Al_2O_3 in Fig. 3(b), but coverages of hundredths of monolayers can still be detected. It is apparent from the increased fractional noise above $\hbar\omega \simeq 8$ eV, where the flux from the synchrotron storage ring falls off, that the sensitivity is photon limited. In practice, the number of photons reaching the detector per point, each taking an acquisition time of 10 sec, was typically between 10^7 and 10^8. This is consistent with the observed noise, which corresponded to fractional reflectivity changes of a few parts in 10^4 at best. Fluctuations arising from orbital instabilities in the radiation source occasionally increased the apparent noise. Tests at fixed wavelength have shown that the chopper itself is stable to ~1 in 10^5 over long time intervals. We therefore expect that very considerable improvements can be made in signal visibility when the new Aladdin ring comes on line, and with improved monochromators. It appears reasonable to expect that the properties of adsorbed atoms can be examined at coverages of $\sim 10^{-3}$ and throughout an energy range extending up to $\hbar\omega \sim 10^3$ eV. Previous differential equipment for use in this energy range has been reported[22] to be stable only to 1 in 10^3, although significantly better stabilities have been achieved below the LiF cutoff.[23]

III. RESULTS

In Figures 4–11, we present differential reflection spectra for Ar and Xe on Al, Mg, and Au, and for Kr on Al and Au at liquid-He temperature. The data are presented in the form, $\Delta R/R\theta$, of fractional reflection changes divided by the coverage (in monolayers), in order that the contribution *per atom* may be compared between films having different thicknesses. For present purposes we define a monolayer as 1.4×10^{15} atoms/cm^2, the close packed (111) surface densities of Au and Al. Observed monolayers of incommensurate Xe on metal single crystals have about half this surface density.[24] The effect of surface roughness of the evaporated films will be to increase the possible density of first-layer adsorbates to a significant but unknown extent. In each of the figures, the sensitivity of the equipment is seen to be adequate for observable signals at coverages <0.1 monolayers. The signals from the metal surfaces are, however, less visible than those from the oxides, particularly for submonolayer coverages. We believe that this is largely due to the fact that the coupling between the first adsorbed layer and the metal broadens the sharp optical structures evident in Figs. 3(a) and 3(b), thereby making these structures significantly less prominent.

In addition to points of detailed interest in each spectrum, one aspect of the composite data has a particular importance that deserves immediate comment. The three cases of Xe on Au and Al and Kr on Au differ significantly from the cases of Ar and Xe on Mg, Ar and Kr on Al, and Ar on Au. This difference arises in the behavior of the main atomic $np^6 \rightarrow np^5\,(n+1)s$ resonance lines as the coverage is reduced below 1 monolayer. In all cases, these spin-orbit split lines are clearly visible for multilayer films as sharp peaks at the threshold of the adsorbate excitation spectrum. In the cases of Xe on Al and of Kr and Xe on Au, however, these excitations are completely eliminated in the submonolayer systems; the adsorbate excitation threshold is shifted to higher energy by several eV. In the remaining five cases the resonance lines stay clearly visible at submonolayer coverages. The lines are broadened, distorted, and perhaps red shifted in most cases, but maintain approximately the same oscillator strength per atom as in the thick films.

We have reported the spectra of Xe on Au and Ti in an earlier publication.[17] Although examined with less sensitivity than is now available, this earlier work showed clearly that the Xe excitons are eliminated from their normal location in these cases, as confirmed for Xe on Au in the present work. In a preliminary, rather sketchy investigation, we have also found that Ne on Al is a case in which the residue of the exciton lines is *not* eliminated at submonolayer coverages. An extensive investigation of rare gases on alkali metals, to be reported elsewhere, has shown that the resonance lines appear clearly at dilute coverages in these cases also. A body of data for a number of different adsorbate-substrate pairs thus establishes a well-defined bimodal behavior of the rare-gas excitation spectra on metals. The detailed explanation of this behavior is the principal topic of Sec. IV. What follows immediately are brief comments on the spectra presented in Figs. 4–11.

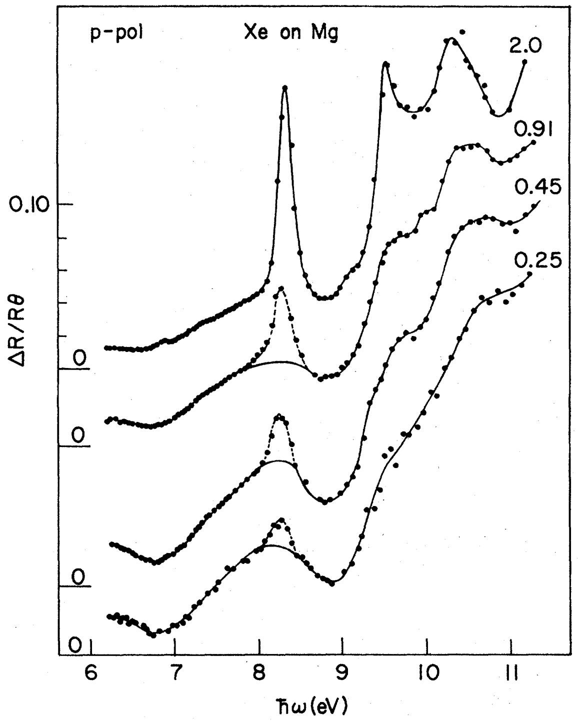

FIG. 4. Normalized reflectivity spectra for Xe adsorbed on Mg (p-polarized light). Broken lines indicate the excitonic resonance contribution.

Xe on Mg (Fig. 4). These data show the excellent noise figures available by differential reflection. It is interesting that the sharp $p^6 \rightarrow p^5 s$ excitation structure characteristic of atomic or solid Xe, which dominates the spectrum for 2.0 monolayers coverage, is not completely eliminated at 0.2 monolayers. The main features of the normalized spectra for coverages of 0.2 and 0.4 monolayers are reassuringly similar to each other, however, as expected if properties of essentially *isolated* adsorbates are being probed. In contrast, the residue of the 8.4-eV peak appears to scale linearly with coverage. The spin-orbit partner of this peak, at about 9.5 eV, decays with decreasing coverage in a similar way, as far as can be judged from the data. We note that the 8.4-eV exciton of the gas phase is replaced in submonolayer results by a structure with an apparent half-width of ~1.0 eV, red shifted by about 0.3 eV from the atomic line, but with a comparable oscillator strength per atom. Above this feature, and at the lowest coverages, the remaining spectrum consists only of a smooth sloping shoulder.

Ar on Mg (Fig. 5). The data for Ar on Mg also show a strong persistence of the atomic resonance line just below 12 eV. In this case the doublet is unresolved, leaving a single asymmetrical peak approximately 1 eV wide at half maximum height.

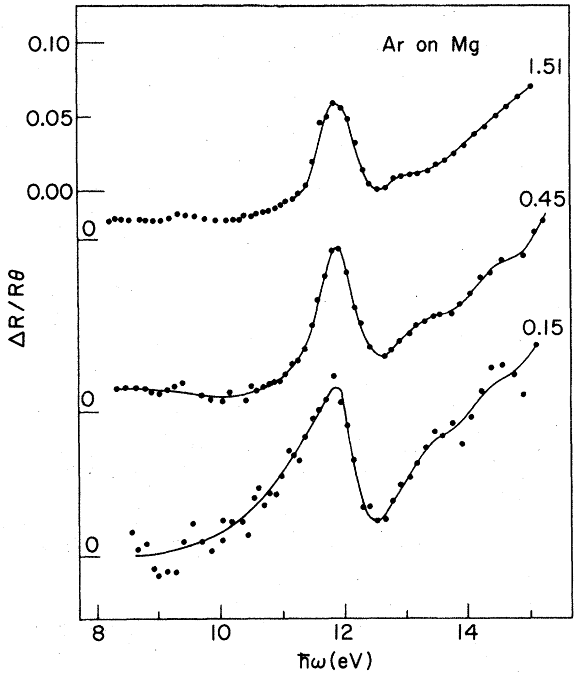

FIG. 5. Normalized reflectivity changes for Ar adsorbed on Mg (p-polarized light).

The shoulder at high energy lacks strongly defined structure.

Kr on Al (Fig. 6). Some of the features observed for Xe and Ar on Mg are apparent for Kr on Al also. The sharp atomic resonance doublet above 10 eV fades rapidly as the coverage falls below monolayer, and cannot be detected at 0.2 monolayers. It leaves a feature having a comparable apparent oscillator strength, almost unshifted, but again of width comparable with 1 eV. The high-energy side is obscured by a shoulder which probably arises from d-like excitations centered near 13 eV. This also broadens as the coverage is reduced.

Ar on Al [Figs. 7(a) and 7(b)]. A much larger ~1-eV apparent red shift of the atomic lines appears in the spectra of Ar on Al taken in p polarization [Fig. 7(a)]. In part this may be illusory, arising from *dispersion*-like distortions of a reflectivity signal which is largely *absorptive* in the other cases. In s polarization [Fig. 7(b)] the low-energy tail is less visible, but poor operating conditions interfered with the signals obtained for low coverages. Both sets of data do, however, show clearly the persistence of a broadened but unweakened evolute of the atomic line near 12 eV, and a shoulder at higher energy whose structure weakens with decreasing adsorbate coverage.

Ar on Au (Fig. 8). These data show a signal strength per adsorbed atom near 12 eV which is substantially reduced as the coverage falls below 1 monolayer. The data in Fig. 8 obtained directly with Ar on Au are not good, owing to larger-than-average noise, but do appear to establish that a nonzero residue of the atomic resonance line persists at submonolayer coverages. The shoulder near 15 eV appears to have a reversed sign in these data, owing to the optical properties of the Au substrate. Both features have been confirmed in a semiquantitative way by additional runs. In an effort to obtain better reflection conditions, the rare gases under observation were adsorbed onto a 50-Å Au film prepared on a freshly evaporated Mg substrate. Both the persistent adsorbate-excitation and the negative-absorption shoulder were reproduced by Ar on Au films only 50-Å thick (i.e., much less than the penetration depth).

Kr on Au (Fig. 9). The distortions produced by Au are apparent in the results for Kr on Au also. In the 4.5 and 2.4 monolayer films the Kr excitons appear as dispersion- rather than absorption-like structures, and the shoulder near 13 eV again appears with reversed sign. As was often the case for Au, the noise from the substrate appears excessive. The most important fact is that the exciton absorption near 10 eV is eliminated, and the oscillator strength evidently blue shifted above 13 eV in submonolayer films. The data establish

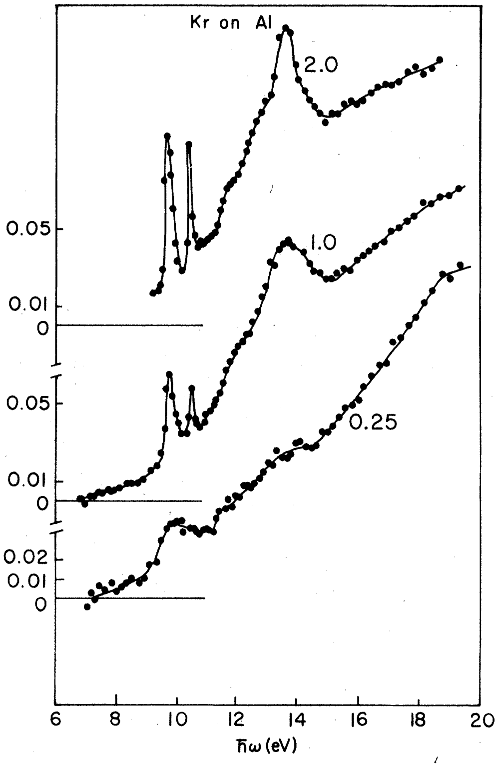

FIG. 6. Normalized reflectivity spectra for Kr adsorbed on Al (p-polarized light).

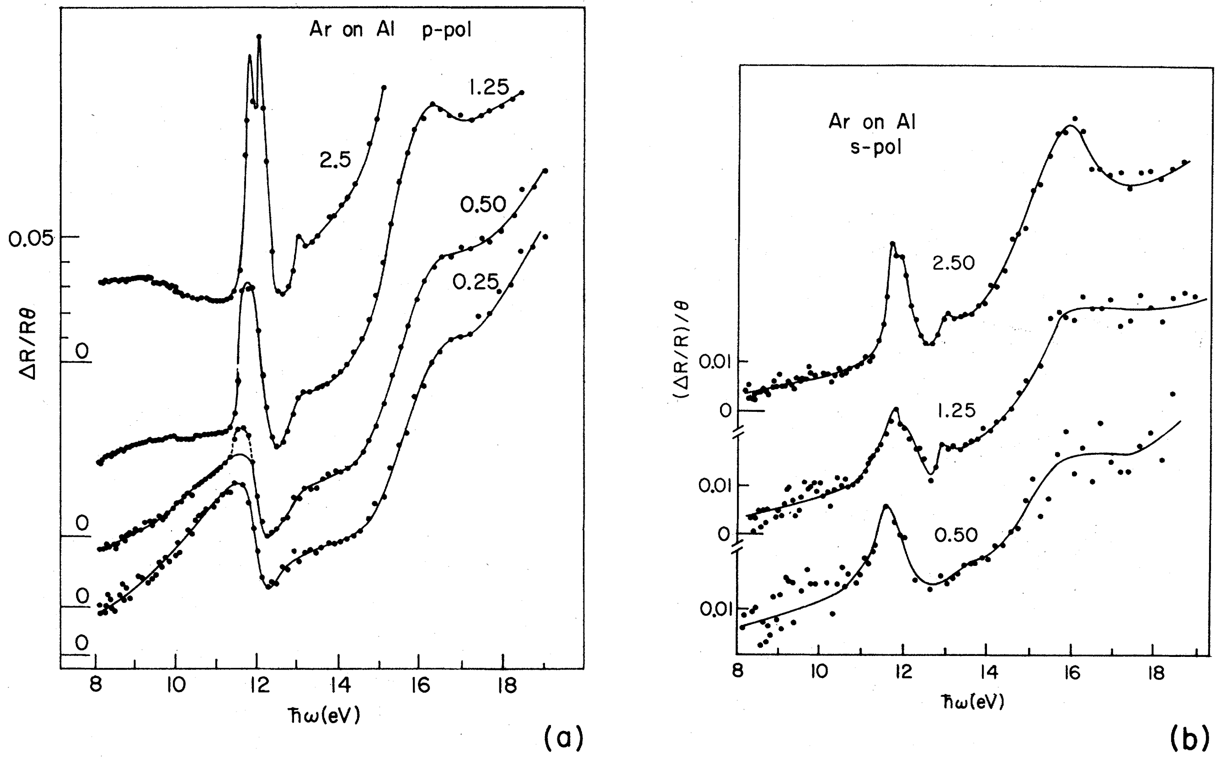

FIG. 7. (a) Normalized reflectivity changes for Ar on Al (p-polarization light). (b) Normalized reflectivity spectra for Ar on Al (s-polarized light).

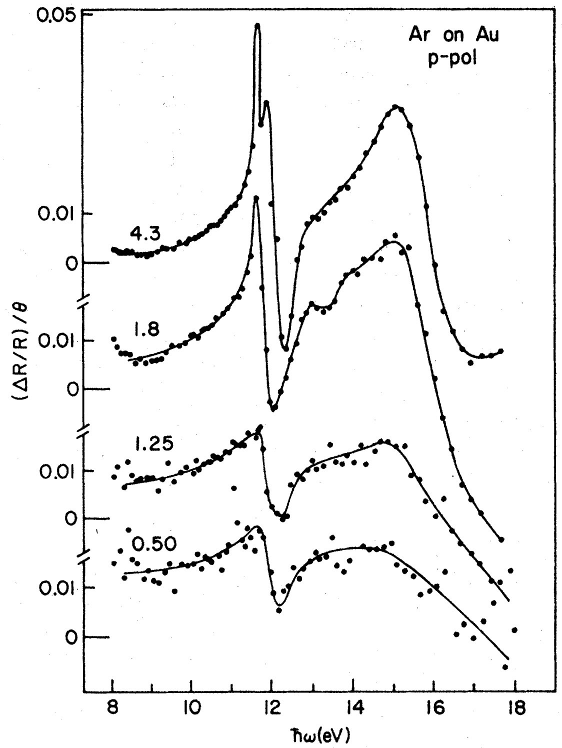

FIG. 8. Normalized reflectivity spectra for Ar adsorbed on Au (p-polarized light).

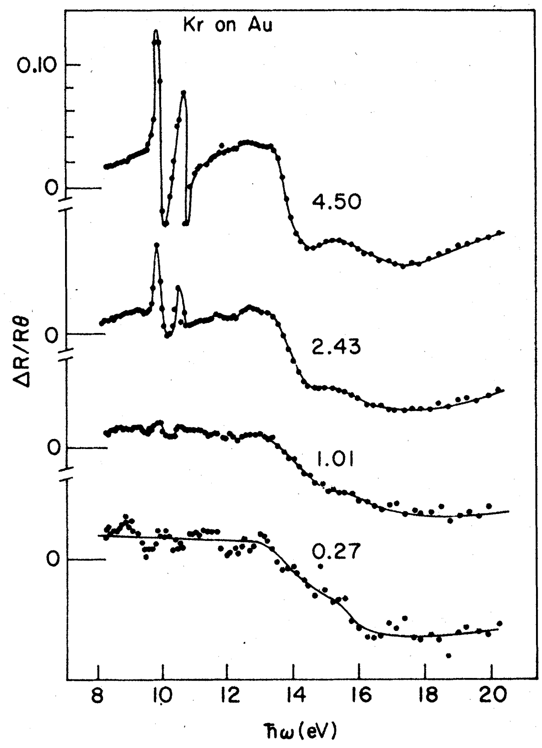

FIG. 9. Normalized reflectivity spectra for Kr adsorbed on Au (p-polarized light).

both the qualitative effect and the large quantitative shift unambiguously.

Xe on Au [Figs. 10(a) and 10(b)]. The data presented here confirm our earlier report[17] that, for submonolayer coverages, the Xe excitons are eliminated on the Au surface. Faint traces of a reverse shoulder above 10 eV can be detected in Fig. 10(a). The wider spectral scan in s polarization [Fig. 10(b)] does reveal minor residual structure near 8 eV at 0.6 monolayers of coverage, and the broad inverted shoulder above 10 eV is once more clearly visible. The complex form of these spectra undoubtedly arises in substantial part from properties of the Au substrate.

Xe on Al (Fig. 11). In this case, also, the sharp, symmetric exciton lines of the multimonolayer system are eliminated as the coverage falls towards 0.7 monolayers. The cause of the gently sloping background from 6 eV upward in energy has not been identified. Rather similar effects observed with CO on Al in p polarization will be reported elsewhere.

IV. DISCUSSION

The detailed quantitative information presented in the spectra of Figs. 3–11 is not yet matched by the theoretical means to derive adsorbate properties from these spectra in a fully quantitative way. Nor, as mentioned in Sec. I, has the theory of the adsorbate-metal surface complex advanced to the point at which the solid-state properties can be predicted accurately from first principles. For these reasons, the present analysis is restricted to qualitative and semiquantitative features of the results. Fortunately, the assembled data allow interpretations of a quite detailed kind. The following discussion focuses on two main features of the data: the bimodal threshold behavior of rare-gas adsorbates at low coverage and the changes that take place in the spectra as the coverage is increased.

A. Threshold at low coverage

1. General properties

In this section we explain why the threshold excitations of rare gases on metals display a bimodal behavior: Some systems exhibit only excitation shoulders, strongly blue shifted (~ several eV) from the expected location of the atomic lines, whereas in other systems the atomic lines persist strongly, are broadened and are often red shifted. No intermediate behavior is observed.

A qualitative explanation follows from two main facts. First, it is well known that alkali atoms become positive ions on certain metallic substrates by transferring their valence electron to

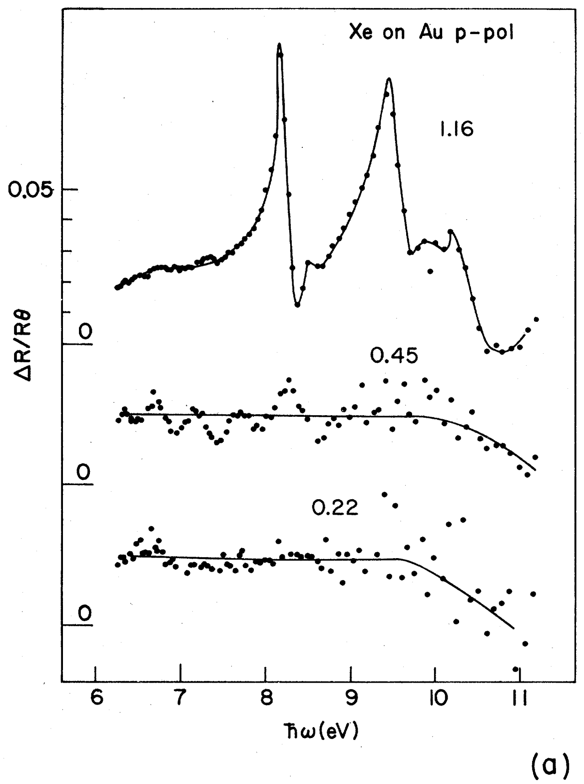

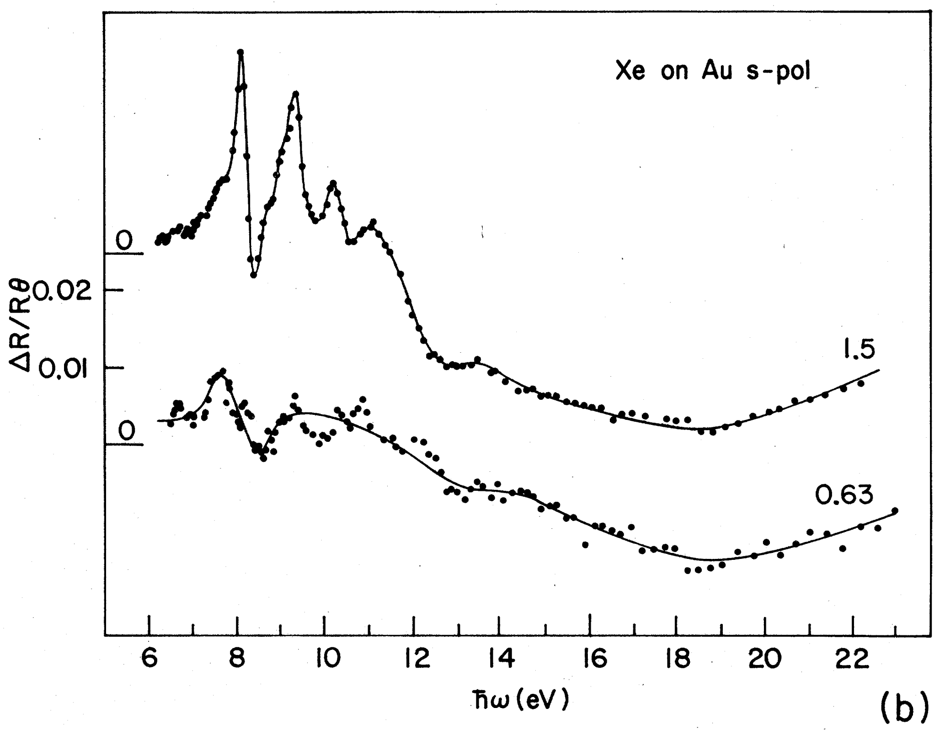

FIG. 10. (a) Normalized reflectivity spectra for Xe adsorbed on Au (p-polarized light). (b) Normalized reflectivity spectra for Xe adsorbed on Au (p-polarized light).

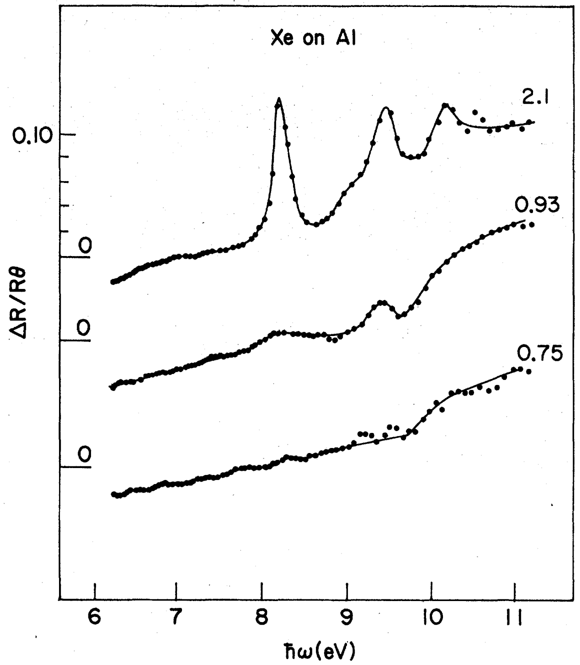

FIG. 11. Normalized reflectivity spectra for Xe adsorbed on Al (p-polarized light).

the underlying metal. To the first approximation this happens when the ionization energy of the atom is less than the work function of the metal (inset, Fig. 12), so that the system lowers its energy when the charge transfer takes place. The electron then localizes in the surface layer near the adsorbate in order to screen the bulk from the ionic field. Second, excited rare-gas atoms in their $np^5(n+1)s$ configurations greatly resemble their neighboring $np^6(n+1)s$ alkali atoms in the Periodic Table. The extra core electron and nuclear charge of the alkali sum to a small pseudopotential which influences the $(n+1)s$ binding energy only by a few percent. The bimodal behavior then arises because excited rare-gas atoms ionize on some surfaces and not on others, just like the alkali ground configuration. The principal determining factor is, once more, a comparison between the work function of the metal and the ionization potential of the excited rare-gas atom.

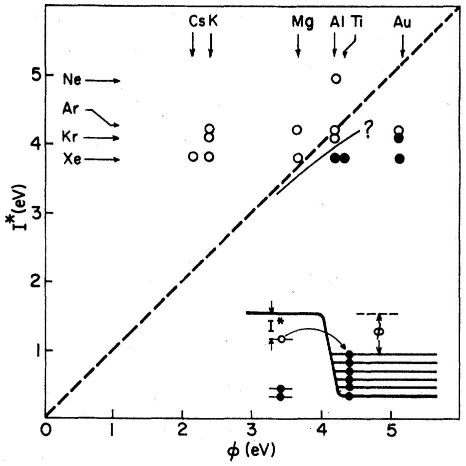

FIG. 12. Systematics of the configurational switching. The ionization energy I^* of the excited configuration and the work function ϕ of the metal are the main determining factors. The broken line $I^*=\phi$ generally separates cases of persistence (open circles) from the cases of charge transfer excitations (solid circles). A rather better separation allows for changes in $I^*-\phi$ caused by atom-substrate interactions (solid line). The charge transfer process is shown inset.

To show how this works out in an almost quantitative way, Fig. 12 (main figure) locates adsorbate-substrate pairs using the excited-adsorbate ionization potential[25] as the ordinate and the work function of the metal[26] as the abscissa. Points representing complexes for which the atomic lines persist are indicated by open circles. Complexes lacking this persistence, and exhibiting instead strongly blue shifted shoulders, are marked by closed circles. Points representing persistent spectra on some alkali-metal substrates, mentioned above, are also included in this figure. The broken line in Fig. 12 represents the locus of complexes with $I^*=\phi$, for which (according to the simplest explanation) the excited rare gas becomes unstable. The solid line identifies a similar locus which exactly separates the full points from the open points. It seems fairly safe to conclude from the similarity between the observed and predicted behavior that the bimodal behavior does indeed reflect an instability of the excited configuration, whereby the work function favors an ionic excited state in some cases and a neutral form in others. Departures of the switch condition from $I^*=\phi$ clearly indicate that the interactions between the two subsystems cause different energy changes of the two alternative configurations. Differences of several tenths of 1 eV would appear reasonable.

The case of Ar on Au in Fig. 12 lies sufficiently far off the line $I^*=\phi$ to cause concern that the observation is in error. Also the data in Fig. 8 for Ar on Au show enough scatter that persistence remains in doubt. For that reason a new investigation of Ar on Au was undertaken using thin Au films (~50 Å) on an Mg substrate to improve operating conditions. These results give a definitive confirmation that the Ar-exciton residue persists in stable form down to 0.2 monolayers. Thus the case of Ar on Au corresponds to a very significant deviation from the broken line in Fig. 12.

An alternative possibility, however, is that the

Au work function is incorrectly represented in Fig. 12. The present films were evaporated onto He temperature substrates. For noble metals this leads to materials with large resistances (~100 $\mu\Omega$ cm/at.%) and hence almost glassy structure. It is therefore possible that ϕ for these films differs significantly from the value in room-temperature films, and that the actual departure from the condition $I^* = \phi$ is smaller at large ϕ than Fig. 12 suggests.

In spite of these systematic deviations, Fig. 12 can probably be used with some confidence to predict results for cases that have not yet been investigated experimentally. For example, it can be predicted that Ar*, Kr*, and Xe* will all ionize on W. We note in addition that the same models also probably describe Ar-like excited molecules such as methane, silane, etc.

2. Threshold energies

In addition to the switch mechanism itself, the actual observations point to certain nontrivial facts concerning the excited configurations in the two distinct cases. These follow from the observed threshold shifts, some of which are rather large, and from the sharpness of the bimodal switching.

Consider first the ionic excited configuration. As mentioned in Sec. I, the optical transition leads directly to a configuration that is self-consistent because the excited-state lifetime certainly exceeds the plasmon period. One can then show that the charge drawn to the surface to screen the ion also causes the large observed blue shifts. In this configuration, a band electron tunneling from the metal into the ion experiences an additional potential energy $V \sim e^2/2z$ caused by the image potential at the ion. This raises the one-electron energy at which a significant occupancy of the ion can occur from $-I$ without the image to $V - I$ with the image. At the same time, the total energy of the excited configuration is lowered by the binding energy E_1 of the ion with the surface, while the ground configuration is lowered by its binding energy E_0. The excitation threshold of the system to the ionic configuration, which occurs at the lowest energy at which electrons penetrate the ion, is therefore

$$\hbar\omega = \hbar\omega_0 + V + E_0 - E_1 ,$$

with $\hbar\omega_0$ the energy of the excitation to the level $-I$ in the free atom.

To make a crude estimate of the shift we neglect E_0, which is merely a polarization bonding, and which probably has its counterpart in E_1. We thus approximate $E_1 - E_0$ by the electrostatic bonding $e^2/4z$ due to the image charge in the excited configuration alone. The predicted blue shift is thus

$$\delta E = \hbar\omega - \hbar\omega_0 = e^2/2z - e^2/4z = e^2/4z .$$

Evidently the blue shifts of the excitation threshold are, to a first approximation, equal in magnitude to the excited-state bonding energy. It is therefore satisfying that the observed shifts have a magnitude of 1.5–3 eV. This is indeed comparable with typical bonding energies of alkali atoms to metallic surfaces upon which they ionize.[27] A somewhat more detailed discussion of ionization has been given by Gadzuk and co-workers.[28] The blue shifts observed in the three cases studied here are collected in Table I.

The energetics of the *neutral* excited configuration can also be approximated by quite simple arguments. The excited and ground states are simply shifted by their interaction energies, E_1 and E_0, with the metal surface. One would normally expect that the metallic bonding of the alkali-like excited state to the surface would exceed the polarization bonding of the ground state. Small red shifts of the optical excitation by a few tenths of 1 eV are therefore not unexpected.

3. The switch mechanism

An interesting aspect of the data is the sharpness of the transition between the two alternative excited configurations. Figure 12 makes evident the fact that the energy balances involved in the switch from one configuration to the other occur on the scale of 0.1 eV in the present work. Work function or ionization potential shifts of this magnitude can apparently switch the system from one excited configuration to the other, and so cause shifts a factor 30 larger in the excitation energy required for the optical threshold. This example clearly emphasizes the distinction between the *total* configurational energies involved in the excitation process and the *one-particle* energies relevant to electron tunneling, to the optical matrix element in the adsorbate cell, and hence to the switch mechanism.

Two related points require additional comment. First, in order that the switch mechanism operates effectively, it is necessary that the neutral excitation does not persist as a resonance beyond the switch condition. This requires that the hopping integral which couples the excited level to

TABLE I. Observed threshold shifts due to ionization compared with the image energy $e^2/4d$.

	Shift (eV)	$e^2/4d$ (eV)
Xe on Au	1.6	1.6
Kr on Au	3.0	1.8
Xe on Al	1.7	1.6

the conduction states be large near E_F, presumably comparable with the one-particle energy shifts which are measured here to be several eV. A magnitude of several eV does not appear unreasonable in the light of the known hopping integrals $\sim E_F = 2-12$ eV that characterize the conduction bands of the metallic substrates used in the experimental work. Second, it may be possible by experiments involving doping with ions to change the work function of a chosen substrate in such a way that the system is swept through the switch condition. Experiments of this type, which could probe *local* work functions and the sharpness of the configurational switchover, are now being undertaken in our laboratories.

4. *Line shapes*

Although the present theoretical capabilities do not warrant a detailed discussion of the observed line shapes, three general observations made in this work are striking enough to focus questions for future work. All concern only the residue of the atomic exciton in the persistent (low ϕ) limit.

First, it is quite noticeable that the persistent line is asymmetrical. It has a long low-energy tail and often a sharp cutoff on the high-energy side. The cases of Xe and Ar on Mg and Ar on Al provide good examples of this behavior. Note that this appears consistent with the notion of a bell-shaped (perhaps Lorentzian) density of one-particle states located on the adsorbed atom in its excited state. In this one-particle picture, the spectrum could thus be explained in a superficial way as derived from transitions originating on a sharp core level and terminating on the bell-shaped density of excited states (but cut off sharply for some reason at high energy). However, a number of arguments lead us to reject this interpretation, at least at its simplest level. Principally, we note that the operation of the switch mechanism demonstrates unequivocally that the many-particle excited configuration determines the response. But in that case the response above threshold must arise from the quasiparticle spectrum of the full excited configuration comprising the conduction band plus the adsorbed atom. This spectrum starts abruptly at E_F with a finite (almost constant) value, rather than exhibiting the extended low-energy tail of the broadened one-particle level. For this reason, the observed line shapes lack a ready explanation.

With this unresolved difficulty we arrive at the second significant observation concerning the line shapes determined in the present work. A ΔSCF (self-consistent fields in both configurations) theory of line shapes near threshold does exist. Until recently, only an asymptotic expression due to the work of Nozières and De Dominicis[29] was available for the line shape near threshold in the bulk metal, but methods introduced by Swartz, Dow, and Flynn[30] now provide exact results for arbitrary energies above threshold. These methods are directly adaptable to surface models.[31] Unfortunately, when developed for conventional conditions these models all generally produce a specific threshold energy followed immediately by intense absorption, as mentioned above. This remains incompatible with the observed Lorentzian-like behavior of the persistent rare gas $p^6 \rightarrow p^5s$ excitations, so an explanation in these terms is lacking.

In this same model, however, the possibility remains that the excited state is magnetic owing to a weak coupling to the electron liquid. We point out elsewhere[31,7] that a magnetic excited state produces a δ-function response of the electronic system, owing to the phase shift of π it introduces at E_F. In this case the observed profile would arise from convolution with the response of other coupled mechanisms. One mechanism, of course, is the excited-state lifetime. The observed broadening corresponds to lifetimes $\sim 10^{-15}$ sec, which is incompatible with the behavior of rare gases in bulk metals, so the lifetime can probably be discounted as a principal cause. A more plausible explanation is the vibrational broadening that arises when the transition occurs at various vibrational coordinates of a weakly bound ground state, so that the spectrum reflects the probable range of excited-state energies for the ground-state vibrational amplitude. This possibility cannot entirely be discounted, but the observed energy range ~ 2 eV appears questionably large.

A third main observation also suggests that phonon broadening cannot be the final explanation of the persistent line shapes. The excited configuration should become more magnetic as the Fermi energy of the substrate metal decreases, owing to the increasing dominance of exchange and Coulomb energies over kinetic energy. Attention thus focuses on alkali-metal substrates, for which the magnetic δ-function response should be best defined, and the overall line shape, therefore, precisely the vibrational spectrum. Our observations of rare-gas spectra on alkali substrates are not yet complete and will be published elsewhere. However, it is already apparent that the spectra have no connection with lattice effects. Rather, we observe for Xe on Cs, for example, a line shape that resembles to a quite unexpected degree the response of Xe at dilution in *bulk* Cs.[32] This latter line is known conclusively to lack extensive phonon broadening.

In summary, the line shapes of persistent rare-gas excitons coupled to metal substrates lack an explanation at present. These are perhaps the simplest of adsorbed species, and the line-shape difficulty therefore points to serious problems in the present understanding of the optical process on surfaces. These phenomena provide interesting challenges for future investigation.

B. Interactions among adsorbates

The method chosen for presenting spectra in Figs. 3–11 is particularly well adapted to the identification of adsorbate-adsorbate interactions. When divided by the coverage, the observed signal then measures the reflectivity change *per adsorbed atom*. This quantity is insensitive to coverage at dilution because, under these conditions, the adsorbates are widely separated on the surface. The changes in spectral profile that take place so strikingly with increasing coverage in Figs. 3–11 therefore probe the interactions among the adsorbed species. Nonlinear optical effects may, in addition, occur for large reflectivity changes $\gtrsim 10\%$, as estimated by the methods of McIntyre and Aspnes.

As an example of spectral dependence on coverage, Fig. 13 shows the absolute heights (i.e., not divided by coverage) of the $P_{3/2}$ and $P_{1/2}$ excitons observed by Cunningham *et al.* for Xe on Au and Ti.[17] The data show clearly that these spectral features originate in the second monolayer alone, since the results extrapolate to zero amplitude near one monolayer of coverage. Results from the present work for Kr on Au, also shown in Fig. 13, exhibit a similar trend.

Figures 14(a) and 14(b) give other results shown, for convenience, as the variation of the *normalized* spectrum $\Delta R/R\theta$ with coverage. The data for Xe on Mg in Fig. 14(a) measure the height of the sharp exciton peak superposed (broken line in Fig. 4) upon the broadened first-layer contribution. The linear variation with coverage of the sharp

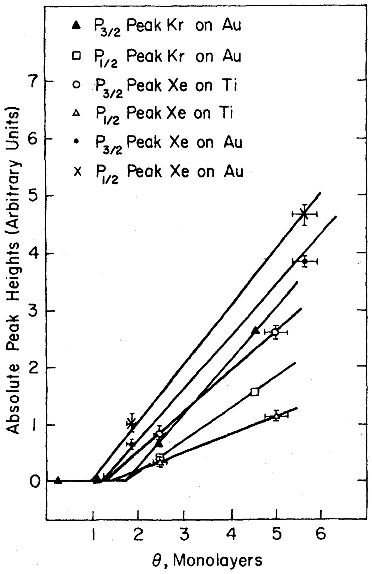

FIG. 13. Absolute peak heights of $p^6 \to p^5 s$ lines for Kr on Au, Xe on Al, and Xe on Au, shown as functions of coverage.

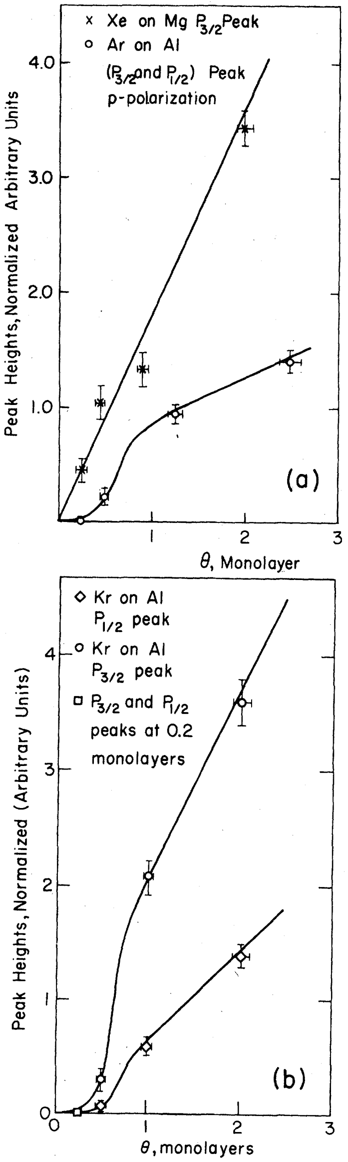

FIG. 14. Normalized peak heights of $p^6 \to p^5 s$ sharp exciton components for (a) Xe on Mg and Ar on Al and (b) Kr on Al, shown as functions of coverage.

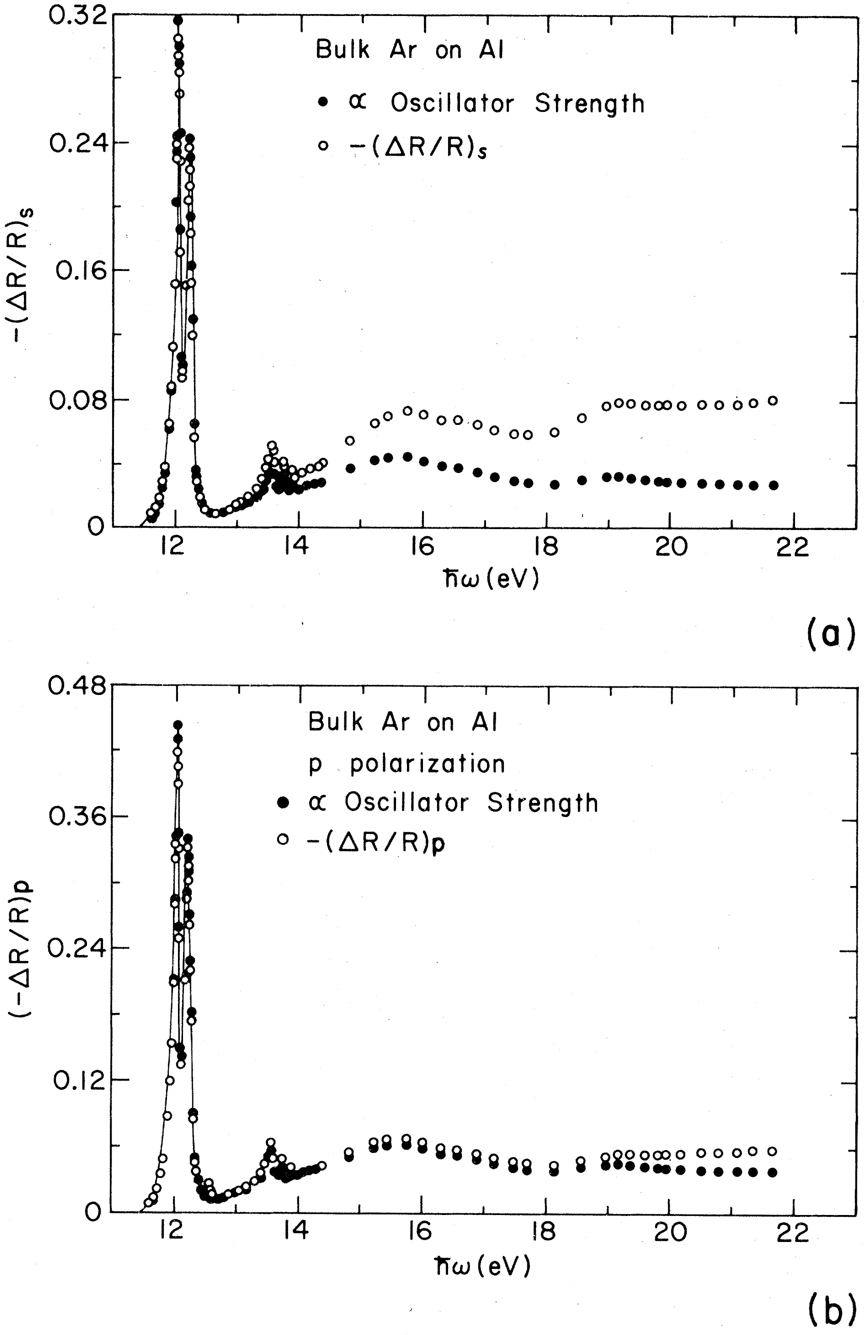

FIG. 15. Predicted spectra according to the McIntyre-Aspnes formula for an Ar monolayer possessing the dielectric properties of solid Ar when placed on a substrate having the dielectric properties of Al. The fractional reflectivity change is compared with the actual oscillator strength for (a) *s* polarization and (b) *p* polarization.

component indicates that it probably arises from Xe *pairs* on the surface. A similar process for Xe pairs in *bulk* alkali-metal–rare-gas alloys has previously been reported.[32] It is believed that the electron and hole resonate together between Xe atoms as a molecular excitation which is rather effectively decoupled from the conduction electrons.

In contrast, the normalized sharp-exciton signals for Ar on Al in Fig. 14(a) and Kr on Al in Fig. 14(b) show a strongly nonlinear variation of amplitude with coverage. This is fitted in the figures by a line proportional to θ^3. A θ^3 coverage dependence, while not established unambiguously by the data, would identify a spectral feature that required four participating adsorbate atoms. Likely candidates are second-layer atoms separated from the substrate by the three first-layer atoms required to form a stable support, the assembly resembling a pyramid. Depolarizing effects on the optical transition, caused by interactions among the adsorbed atoms, would produce effects similar to those observed but with a $\theta^{3/2}$ coverage dependence of the unnormalized signal.[33] This mechanism involves the enhancement of the residual line at high coverage by the effect of other rare-gas atoms in decreasing the work function. In practice, no signs of $\theta^{3/2}$ coverage dependences are visible and this mechanism therefore has no apparent importance for the cases studied so far.

ACKNOWLEDGMENTS

The authors wish to thank Dr. J. L. Erskine and Mr. D. Gibbs for advice and for assistance with the experiments. The staff of the Synchrotron Radiation Center at Stoughton, Wisconsin provided helpful services without which this work could not be completed. Professor W. L. McMillan has given assistance with computer programming, and Professor G. Ehrlich has supplied helpful references. The work was supported in part (J.A.C.) by the National Science Foundation under Grant No. DMR-77-27942 and (D.K.G.) by the University of Illinois MRL Grant No. DMR-77-23999.

APPENDIX: THE McINTYRE-ASPNES ANALYSIS

While the formulation of the reflectivity as a classical sharp-boundary problem cannot be fully justified, the results nevertheless have a significant semiquantitative value. It is therefore useful to gauge how faithfully the spectral features actually observed in reflection track the optical absorption coefficient expected of the adsorbates. An example has been carried through in Figs. 15(a) and 15(b). Here, an Ar layer on Al is modelled using the MA expressions for the known dielectric properties of the Al substrate and the properties of bulk Ar representing the dielectric layer. Figure 15(a) compares the calculated s-polarized differential reflectivity with the Ar bulk oscillator strength, both as functions of photon energy in the relevant energy range. Similar results for p-polarized light are given in Fig. 15(b). In both cases, the oscillator strength is scaled to fit the reflectivity change at the first exciton line.

For both s- and p-polarized light the reflection spectra do follow the oscillator strength in a semiquantitative way. In both cases the reflectivity appears to be enhanced relative to the oscillator strength at high energy. This distortion is much larger in s than in p polarization. Some significance is therefore added to the fact that the actual reflectivity data for Ar on Al show an effect at high energy in p-polarized light that is considerably larger than that in s-polarized light [Figs. 7(a) and 7(b)].

We report briefly some further efforts to use the MA formulation to interpret the data directly. A use of data for both s- and p-polarized light in an attempt to obtain the substrate dielectric function unambiguously encountered difficulties with the fact that only imaginary solutions would be obtained in certain energy ranges. Similar problems have been reported by others. Lorenzian fits to the data invariably yielded continuous values of both the imaginary and real parts of the dielectric constant, but the values derived from s- and p-polarized data differed markedly. It should be noted that the main spectral features reproduce quite adequately in all cases, but in distorted form.

---

[1] G. Ehrlich and F. G. Hudda, J. Chem. Phys. 30, 493 (1959).

[2] R. Gomer, Aust. J. Phys. 13, 391 (1960).

[3] J. C. P. Mignolet, J. Chem. Phys. 21, 1298 (1953);

[4] See, e.g, T. Engel and R. Gomer, Chem. Phys. 52, 5572 (1970).

[5] For a discussion and references see B. E. Nieuwenhuys, O. G. Van Aardenne, and W. M. H. Sachtler, Chem. Phys. 5, 418 (1974).

[6] A useful account is given by C. Mavroyannis, Mol. Phys. 6, 593 (1963).

[7] A brief summary of this work is given by J. A. Cunningham, D. K. Greenlaw, C. P. Flynn, and J. L. Erskine, Phys. Rev. Lett. 42, 328 (1979). A somewhat different type of rare-gas level shift in photoemission has recently been reported by J. Kappas, F. Nitschke, K. Wandelt, and G. Erhl, Surf. Sci. 88, 1 (1979).

[8] R. Avci and C. P. Flynn, Phys. Rev. Lett. 41, 428 (1978).

[9] K. Horn, M. Scheffler and A. M. Bradshaw, Phys. Rev. Lett. 41, 822 (1978); for earlier work on W see B. J. Waclawski and J. F. Herbst, Phys. Rev. Lett. 35, 1594 (1975); J. F. Herbst, Phys. Rev. B 15, 3720 (1977).

[10] J. B. Taylor and I. Langmuir, Phys. Rev. 44, 423 (1933).

[11] N. D. Lang and W. Kohn, Phys. Rev. B 3, 1215 (1971).

[12] For a comprehensive review of this area see N. D. Lang, in *Solid State Physics*, edited by H. Ehrenreich, F. Seitz, and D. Turnbull (Academic, New York, 1973), Vol. 28.

[13] N. D. Lang, Phys. Rev. B 4, 4234 (1974); N. D. Lang

and A. R. Williams, Phys. Rev. B 18, 616 (1978).

[14] See, e.g., A. B. Kunz and D. L. Klein, Phys. Rev. B 17, 4614 (1978).

[15] G. T. Surratt and A. B. Kunz, Phys. Rev. B 19, 2352 (1979).

[16] C. P. Flynn and N. O. Lipari, Phys. Rev. B 7, 2215 (1973).

[17] J. A. Cunningham, D. K. Greenlaw, P. M. Layton, J. L. Erskine, and C. P. Flynn, J. Phys. F 7, L281 (1977).

[18] J. D. E. McIntyre and D. E. Aspnes, Surf. Sci. 24, 417 (1971).

[19] J. B. Restorff and H. D. Drew (unpublished); M. A. Passler and P. J. Stiles, J. Vac. Sci. Technol. 15, 2 (1978); J. Anderson, G. W. Rubloff, M. A. Passler, and P. J. Stiles, Phys. Rev. B 10, 2401 (1974); R. E. Prange, H. D. Drew, and J. B. Restorff, J. Phys. C 10, 5083 (1977).

[20] P. J. Feibelman, Phys. Rev. B 12, 1319 (1975); 14, 762 (1976).

[21] See, e.g., R. A. Tilton, thesis, University of Illinois, 1975 (unpublished).

[22] See, e.g., W. Gudata, C. Kunz, and J. Karlan, Appl. Opt. 13, 1412 (1974).

[23] See, e.g., G. W. Rubloff, J. Anderson, M. A. Passler, and P. J. Stiles, Phys. Rev. B 10, 2401 (1974).

[24] See, e.g., H. Papp and J. Pritchard, Surf. Sci. 53, 371 (1975) for Xe on Cu, and G. McElhiney, H. Papp, and J. Pritchard, Surf. Sci. 54, 617 (1976) for Xe on Ag.

[25] See, e.g., C. E.Moore, Atomic Energy Levels, NBS (1971).

[26] For Au and Ti, see the collection of data by D. E. Eastman, Phys. Rev. B 2, 1 (1970); for other cases the values selected by N. D. Lang and W.Kohn, Phys. Rev. B 3, 1215 (1971) are used.

[27] For a discussion and some references see R. Gomer, in *Solid State Physics*, edited by H. Ehrenreich, F. Seitz, and D. Turnbull (Academic, New York, 1975), Vol. 30.

[28] J. W. Gadzuk, Surf. Sci. 6, 133 (1967); see also N. D. Lang and A. R. Williams (Ref. 13).

[29] P. Nozières and C. T. De Dominicis, Phys. Rev. 173, 1097 (1969).

[30] C. Swarts, J. D. Dow, and C. P. Flynn, Phys. Rev. Lett. 43, 158 (1979); J. D. Dow and C. P. Flynn, J. Phys. C 13, 1341 (1980).

[31] C. P. Flynn, Phys. Rev. B 14, 5294 (1976).

[32] D. J. Phelps, R. A. Tilton, and C. P. Flynn, Phys. Rev. B 14, 5254 (1976).

[33] J. Topping, Proc. Roy. Soc. A114, 67 (1927).